doi: 10.18323/2782-4039-2023-1-23-32

Numerical modeling of temperature fields during friction stir welding of the AA5083 aluminum alloy

Igor N. Zybin*[1], PhD (Engineering), Associate Professor,
assistant professor of Chair "Material Bonding and Processing Technology"
Mikhail S. Antokhin[2], graduate student of Chair "Material Bonding and Processing Technology"
Kaluga Branch of Bauman Moscow State Technical University, Kaluga (Russia)

***E-mail: igor.zybin@mail.ru**

[1]ORCID: https://orcid.org/0000-0002-5738-4231
[2]ORCID: https://orcid.org/0000-0002-8043-1606

Received 12.12.2022 *Accepted 30.01.2023*

Abstract: One of the important parameters ensuring the production of a welded joint without continuity defects during friction stir welding is the provision of the required temperature in the metal bonding zone. Significant difficulties arise when determining experimentally the temperature directly in the stir zone of metals using thermocouples. In this regard, the application of numerical methods describing the distribution of temperature fields during friction stir welding is relevant. In the work, numerical modeling of temperature fields during friction stir welding was used, which was based on the finite element method using Abaqus/Explicit software. Modeling was carried out taking into account the coupled Euler – Lagrange approach, the Johnson – Cook plasticity model, and the Coulomb friction law. Using the finite element method, the models of a part, substrate, and tool were constructed taking into account their thermophysical properties. To reduce the computation time, an approach based on the metal mass scaling by recalculating the density of the metal and its thermal properties was used. The authors matched coefficients of scaling of the material mass and heat capacity for the selected welding mode parameters. To evaluate the validity of the results of numerical modeling of temperature fields during friction stir welding, the experimental research of the temperature fields using thermocouples was carried out. The paper shows the possibility of numerical modeling of temperature fields during friction stir welding with the help of the coupled Euler – Lagrange approach and Abaqus/Explicit software. Due to the application of the approach associated with material mass scaling, the calculation time is reduced by more than 10 times.

Keywords: friction stir welding; AA5083; coupled Euler – Lagrange approach; numerical modeling of temperature fields.

For citation: Zybin I.N., Antokhin M.S. Numerical modeling of temperature fields during friction stir welding of the AA5083 aluminum alloy. *Frontier Materials & Technologies*, 2023, no. 1, pp. 23–32. DOI: 10.18323/2782-4039-2023-1-23-32.

INTRODUCTION

Friction stir welding (FSW) is one of the modern and advanced methods for producing goods from aluminum alloys. The formation of a welded joint is carried out in the solid phase without melting the parts to be joined, which is the advantage of this method compared to the traditional arc welding methods. The strength of welded joints produced by FSW, as a rule, is 90–95 % of the base metal strength [1–3]; however, it can reach the strength of the base metal as well. Bending tests show that the destruction of welded samples occurs along the base metal [1].

The main parameters of the process, characterizing the welded joint formation during FSW without defects include the provision of the required temperature in the welding zone. The base amount of heat is released as a result of friction of a tool with the parts to be welded. In this case, the amount of heat released during welding affects the seam structure, the width of a heat-affected zone and the welded joint quality. The geometric shape of a tool pin significantly influences the processes of heat generation.

To determine the temperatures in the metal joining zone during FSW, experimental and theoretical studies are used. Thermocouples are widely used in experimental studies. At the same time, it is virtually impossible to determine the temperature using thermocouples directly in the mixing zone of metals. Moreover, such studies require significant time expenditures (thermocouples preparation and fullering). In this regard, the numerical methods are widely used to study the distribution of temperature fields during FSW. As a rule, these methods are based on the use of the finite element method.

Finite element models used in FSW can be divided into three types: thermal, thermomechanical without flow, and thermomechanical models with flow. According to the Lagrange approach, in the models with flow, the elements can be strongly distorted and the final results may be inaccurate. To avoid grid distortion, several modelling methods are used: the adaptive model grid refinement and the arbitrary Euler – Lagrange approach. The flow-based models are developed using the computational fluid dynamics software systems. The impossibility to take into account the hardening of the material is a disadvantage of this method, since here a rigid-viscous-plastic material is considered.

The flow-based models are also developed using the coupled Euler – Lagrange approach [4–6]. This method of analysis combines two approaches: Euler's and

Lagrange's. A tool is modeled as a rigid isothermal Lagrange body, and has a "reference point" control point, and a part is modelled using the Euler approach. With the help of a contact, the direct interaction of a tool and a part is simulated [6]. The works [7; 8] prove the efficiency of applying the coupled Euler – Lagrange approach when modelling the FSW process. Therefore, to obtain proper results when studying the distribution of temperature fields during FSW, the coupled Euler – Lagrange approach should be used. However, one should take into account the change in the material thermophysical properties depending on the temperature [9; 10], and the Johnson – Cook material plasticity model, the utilization efficiency of which is proved by the results of experimental tests in the work [11] during the numerical modelling of the FSW process.

The FSW studies are carried out in various commercial software, such as: ABAQUS, DEFORM-3D, ANSYS, FORGE 3, LS-DYNA. However, the thermomechanical models built in DEFORM-3D and ABAQUS turned out to be better than the models built in other software, which allowed obtaining a theoretical distribution of temperature fields relevant to the experimental data.

It is also important to significantly reduce the time of theoretical calculations when developing a model, since such calculations can take up to 500 hours or more, depending on the personal computer capabilities, the task complexity, and the weld length. To reduce the calculation time, two approaches are used: "Time Scaling" and "Mass Scaling" under the condition that the deformation rates and inertial forces remain small. Mass scaling is carried out by recalculating the metal density. Time scaling is carried out by replacing the time with a fictitious variable. However, in both cases, to maintain the proper distribution and take into account the heating temperature, the material thermal properties are recalculated. These approaches allow saving the calculation time without the loss of the result accuracy.

The study is aimed at the computer simulation of the distribution of temperature fields during FSW of the AA5083 aluminum alloy, based on the coupled Euler – Lagrange approach, which reduces the time of theoretical calculations virtually with no loss of their accuracy.

METHODS

Modelling of the distribution of temperature fields during welding of the AA5083 aluminum alloy was carried out in the Abaqus/Explicit software product. The model was based on the coupled Euler – Lagrange approach and on an explicit integration scheme designed to calculate non-stationary dynamics, quasi-statics, and rapid processes. The Abaqus/Explicit software product allows applying the Coulomb friction law, the Johnson – Cook material plasticity model, and includes discontinuous nonlinear behaviour.

To simulate the temperature fields during FSW, a joint solution of strength and fluid dynamics tasks is used – the coupled Euler – Lagrange approach in a three-dimensional formulation [12; 13]. This method allows simulating fluid dynamics tasks on the Euler grids and dynamic strength problems on the Lagrange grid within a single spatial solution.

The model included a part, a substrate, and a tool. In this respect, the material of the part and the substrate was modelled within the Euler approach, and the tool material was modelled within the Lagrange approach [14]. The peculiarity of such simulation is that the generation of a finite element grid on the part and substrate was performed only on the area constructed within the Euler approach.

The Lagrange grid nodes are connected to the material. The model grid elements and the boundaries of these grid elements coinciding with the boundaries of the material are deformed under the force action. The Lagrange grid elements themselves are filled with the material. The finite element models of the part, substrate, and the tool with the substrate were constructed using the EC3D8RT and C3D8RT elements, respectively, which are three-dimensional eight-node elements. In the nodes of model elements, four degrees of freedom were available: movements along three mutually perpendicular axes and the temperature degree of freedom.

The contact between the model elements took into account the Coulomb friction law, where the sliding friction force is proportional to the normal force acting between the bodies. The sliding friction coefficient for a metal-metal pair is usually in the range of 0.15–0.3. Within the numerical modelling, its value, as a rule, is assumed to be constant [15]. To simulate the distribution of temperature fields, the sliding friction coefficient was chosen to be 0.15.

Modelling of the distribution of temperature fields was performed for the base metal in the form of a sheet of the AA5083 alloy 5 mm thick. An AISI 1020 steel sheet 10 mm thick was chosen as a substrate material. The welding mode was chosen taking into account the absence of continuity defects in the welding zone: the tool rotation speed is 560 rpm, the welding speed (the longitudinal tool feed) is 40 mm/min. The angle of tool inclination to the vertical was 2°. The depth of penetration of a tool shoulder into the part is 0.1 mm. The geometric dimensions of the tool are shown in Fig. 1.

Fig. 2 shows the models of a part with a substrate and a tool constructed using the finite element method. The model of the part with a substrate included 6000 elements, and the model of the tool – 2741 elements.

To account for the plastic deformation of the model elements, the empirical Johnson – Cook plasticity model was used, which took into account kinematic hardening, the effects of isotropic hardening, the deformed metal adiabatic heating, and the temperature changes. In this model, the yield strength is determined by the following formula [16; 17]:

$$\sigma_y = \left[A + B \cdot \varepsilon_p^n \right] \cdot \left[1 + C \cdot \ln\left(\frac{\varepsilon_p^n}{\varepsilon_0} \right) \right] \cdot \left[1 - \left(\frac{T - T_r}{T_m - T_r} \right)^m \right], \quad (1)$$

where σ_y – is the yield strength;

ε_p^n – is the effective plastic strain;

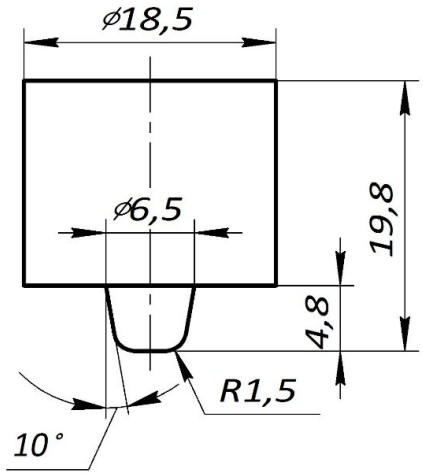

Fig. 1. *FSW tool dimensions*
Рис. 1. *Размеры инструмента для СТП*

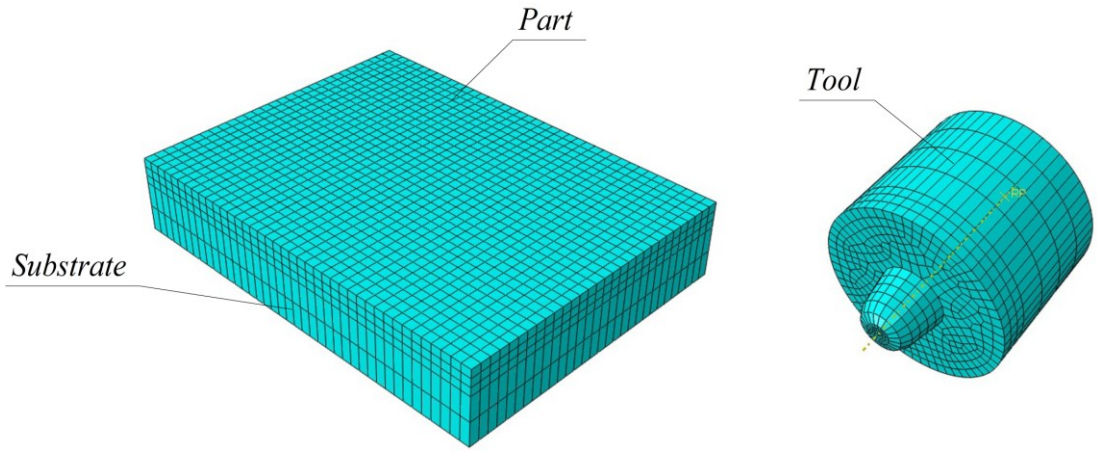

Fig. 2. *Finite element models of the part, substrate, and tool*
Рис. 2. *Модели детали, подложки и инструмента, построенные с помощью метода конечных элементов*

T_m – is the melting temperature;
T_r – is the room temperature;
T – is the material temperature;
A, B, C, n, m, ε_0 – are the model parameters.

The model parameters (1) are shown in Table 1.

In the current work, an approach related to metal mass scaling is selected to reduce the calculation time.

The metal density was calculated as per the formula

$$\rho^* = k_m \cdot \rho \,, \qquad (2)$$

where ρ^* – is the fictitious density;
k_m – is the scaling ratio determining what fold approximately the calculation time will be reduced (k_m>1);
ρ – the material density.

The scaling ratio k_m is chosen so that the inertial forces on the right side of an equation (2) remain small.

The scaling ratio value is chosen equal to k_m=400. When solving the formulated task, the Navier thermoelasticity equation is used:

$$\mu \cdot \nabla^2 \cdot u + (\lambda + \mu) \cdot \nabla \cdot tr(E) - \alpha \cdot \lambda \cdot \nabla \cdot T = \rho \cdot \frac{\partial u}{\partial t^2} \,, \qquad (3)$$

where E – is the linear strain tensor;
μ and λ – are the Lame coefficients;
T – is the temperature;
α – is the thermal expansion coefficient;
u – is the displacement vector;
ρ – is the density;
t – is the time;
∇ – is the nabla operator;
tr – is the E matrix trace.

When replacing the density with a fictitious one, thermal constants change. The influence of this effect was compensated by recalculating the material heating capacity as per the formula

$$c_e^* = c_e \cdot k_n^{-1}, \quad (4)$$

where c_e* – is the fictitious density;
k_n – is the heating capacity scaling ratio;
c_e – is the material heating capacity.

Since the value of the right side of the equation (3) has increased, the minimum stable time increment of the explicit solver increases [23].

The heating capacity scaling factor k_n was selected to reduce the calculation time, while providing the accuracy comparable to that when simulating the distribution of temperature fields without the metal mass scaling. The heating capacity scaling ratio k_n was assumed to be equal to the mass scaling factor k_m=400.

To verify the validity of the computer simulation results, the authors carried out an experiment on butt welding of two parts 5 mm thick made of the AA5083 aluminium alloy. Welding was performed on a FSS400R vertical turning mill using a tool, the geometric dimensions of which are shown in Fig. 1. The tool was made of H13 tool die steel. The tool hardness was 53…57 HRC after quenching in oil and next tempering. To study temperature fields, the authors used a LTR modular data acquisition system with an LGraph2 multichannel recorder and a K-type thermocouple (chromel-alumel).

A thermocouple layout is shown in Fig. 3. To improve the accuracy of the results of obtaining the distribution of temperature fields, two groups of thermocouples were prepared.

RESULTS

The temperature distribution on the surface of welded parts during computer simulation of the FSW process without mass scaling and with scaling (k_m=k_n=400) is shown in Fig. 4.

From Fig. 4, it is evident that with the selected scaling factors, the distribution of temperature fields differs significantly. Therefore, it was necessary to update the scaling factor k_n. Based on the comparative analysis of the obtained temperature fields without and with scaling, the heating capacity scaling ratio was assumed to be 257. After that, the simulation of the temperature fields' distribution was repeated. Fig. 5 shows the temperature distribution on the surface of welded parts during computer simulation of the FSW process without mass scaling and with scaling (k_m=400; k_n=257). According to the simulation results, the welding area maximum temperature was 584 °C.

Fig. 6 shows the location of thermocouples before welding (a) and after welding (b) of parts during the investigational study when producing a butt welded joint.

The results of the investigational study are shown in Fig. 7.

Fig. 8 presents the experimental data and data obtained during numerical modelling for the considered points of installing the 1 and 2 thermocouples.

DISCUSSION

The analysis of the obtained distribution of temperature fields presented in Fig. 5 showed a slight difference between this distribution when using mass scaling and without scaling. With the selected scaling factors, the distribution of isotherms differs by no more than 6 %. In this case, the calculation time was reduced from 600–700 hours (approximate value) to 60 hours.

The maximum temperature values in the welding area obtained in this work as a result of numerical modeling (584 °C) are in good agreement with data of some works where the FSW process simulation was performed. In particular, in the work [19], during numerical modelling of temperature fields when producing a FSW butt joint, the maximum temperature in the welding area was 585 °C. When obtaining T-formed welded joints as a result of the FSW process numerical modelling based on the Euler –

Table 1. *The values of the parameters of the Johnson – Cook plasticity model for the AA5083 and AISI 1020 materials [18]*
Таблица 1. *Значения параметров модели пластичности Джонсона – Кука для материалов AA5083 и AISI 1020 [18]*

Parameter	Material	
	AA5083	AISI 1020
A	137.9	187.60
B	216.73	199.10
n	0.4845	0.1717
m	1.2250	0.4437
T_m	659.85	1460.00
T_r	25	25

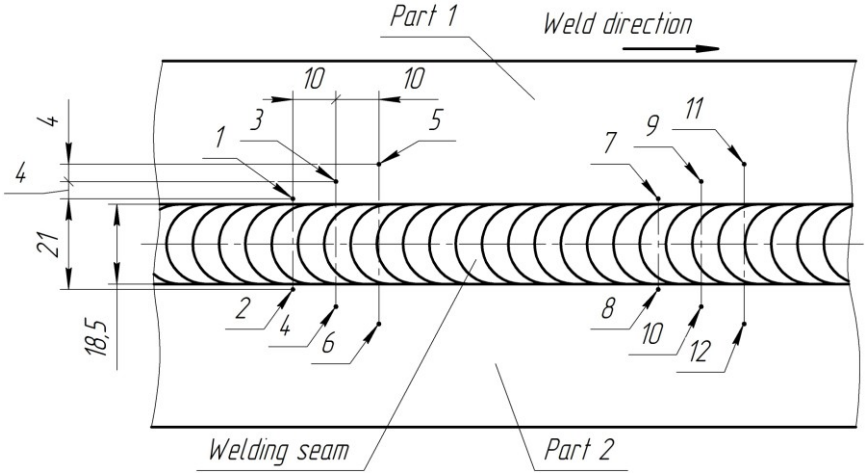

Fig. 3. *A thermocouples layout: 1–12 – thermocouples installation locations*
Рис. 3. *Схема расположения термопар: 1–12 – места установки термопар*

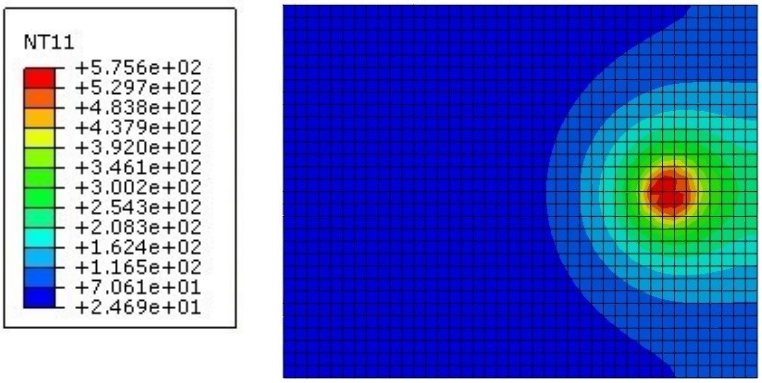

a

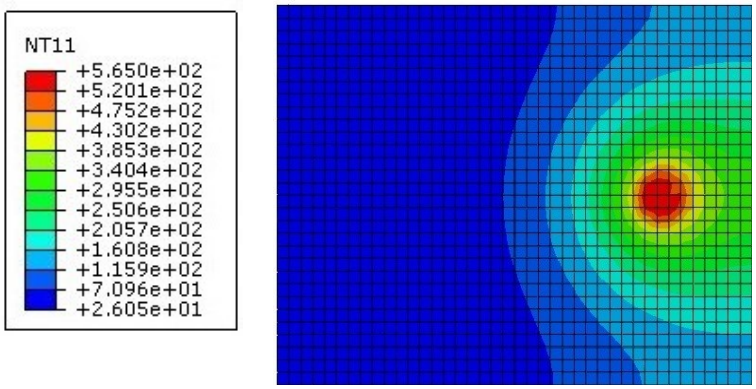

b

Fig. 4. *Temperature fields distribution on the surface of welded parts when modeling the FSW process:*
a *– a model without mass scaling;* ***b*** *– a model with mass scaling (k_m=k_n=400)*
Рис. 4. *Распределение температурных полей на поверхности свариваемых деталей при моделировании процесса СТП:*
a *– модель без применения масштабирования массы;*
b *– модель с применением масштабирования массы (k_m=k_n=400)*

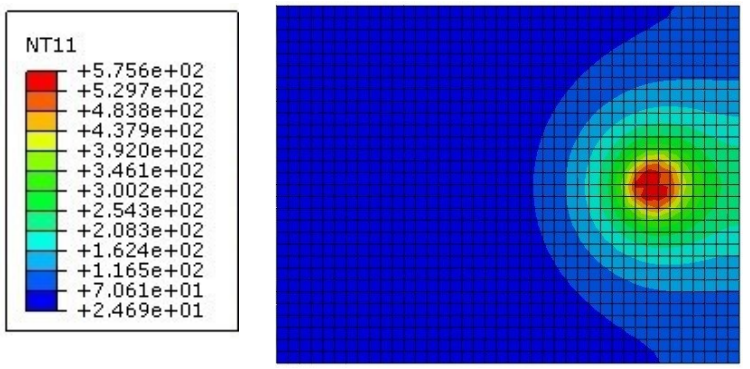

a

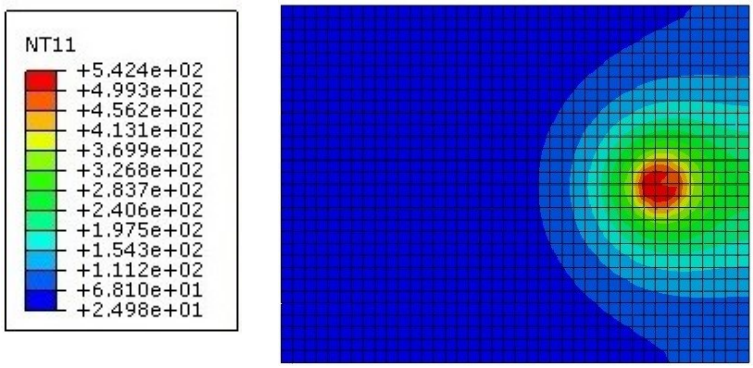

b

Fig. 5. *Temperature fields distribution on the surface of welded parts when modeling the FSW process:*
a *– a model without mass scaling;* ***b*** *– a model with mass scaling (k_m=400; k_n=257)*
Рис. 5. *Распределение температурных полей на поверхности свариваемых деталей при моделировании процесса СТП:*
a *– модель без применения масштабирования массы;*
b *– модель с применением масштабирования массы (k_m=400; k_n=257)*

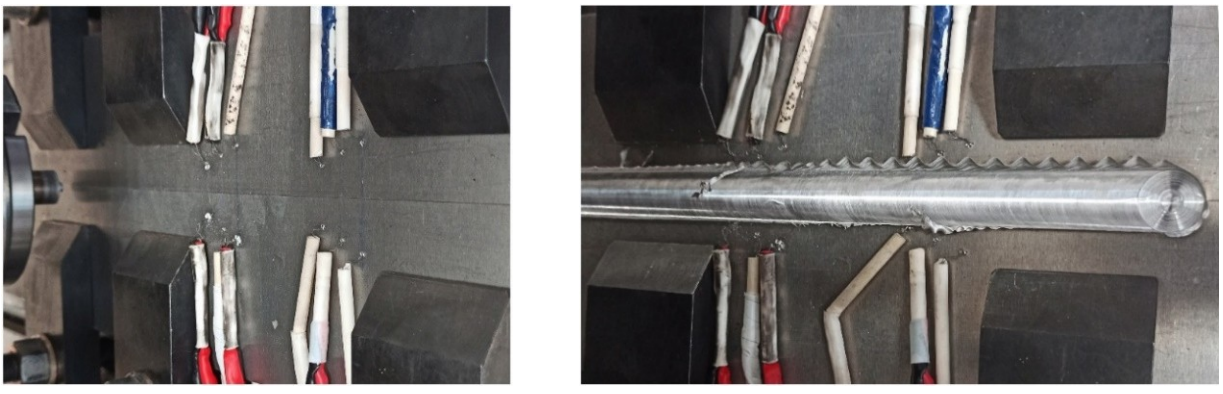

a ***b***

Fig. 6. *The location of thermocouples before (**a**) and after (**b**) welding of parts*
Рис. 6. *Расположение термопар перед (**a**) и после (**b**) сварки деталей*

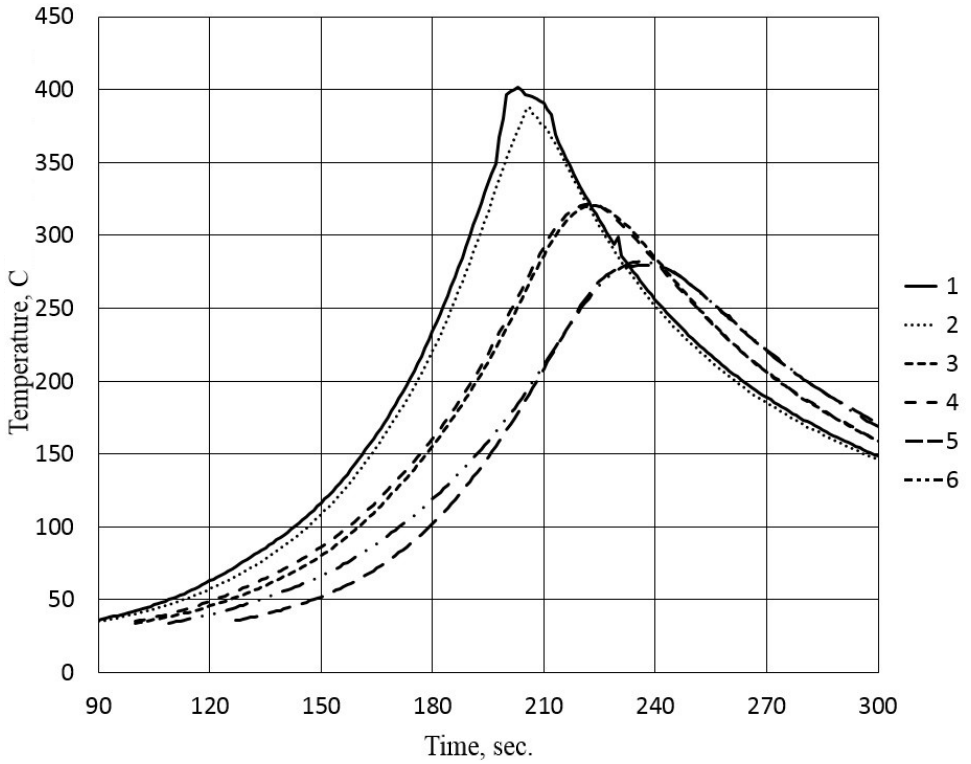

Fig. 7. *The distribution of temperature fields during friction stir welding: 1–6 – the numbers of thermocouples*
Рис. 7. *Распределение температурных полей при СТП: 1–6 – номера термопар*

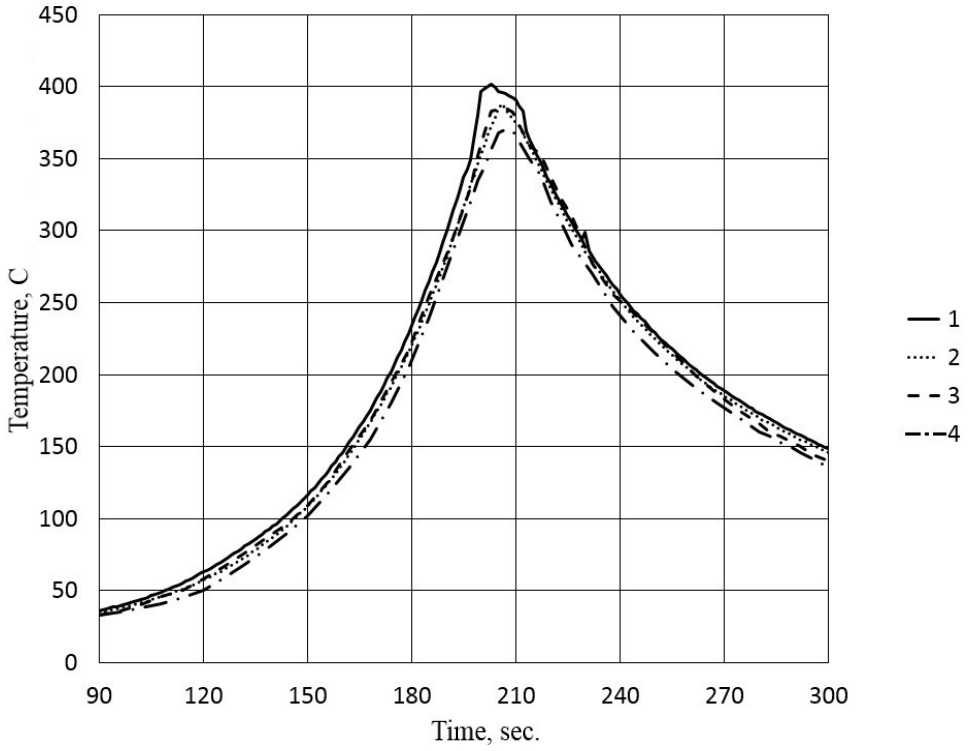

Fig. 8. *The distribution of temperature fields during friction stir welding obtained by computer modeling and experimentally:*
1–2 – thermocouples (an experiment); 3–4 – thermocouples (modeling)
Рис. 8. *Распределение температурных полей при СТП, полученных с помощью компьютерного моделирования и экспериментальным путем:*
1–2 – термопары (эксперимент); 3–4 – термопары (моделирование)

Lagrange approach, in the work [20], the maximum temperature in the welding area was 575 °C.

At the periphery of the tool-part contact during welding (thermocouples 1 and 2, Fig. 7), the maximum temperature on the surface of the part on the side of the tool backward slip zone is higher than on the side of the running-on zone. This is explained by the fact that an overpressure zone appears in front of the tool on the side of the running-on zone. From this zone, the tool working surface displaces metal, which is in the plastic state and prevents the tool movement, due to its translational-rotational movement, into the zone located behind the tool, i.e. into the backward slip zone.

MAIN RESULTS AND CONCLUSIONS

The analysis of the results of experimental investigations showed that at the periphery of the tool-part contact during welding (thermocouples 1 and 2), the maximum temperature reaches 401.6 °C, and the temperature on the part surface on the side of the tool backward slip zone is approximately 14 °C higher than on the side of the tool running-on zone. It is associated with different conditions of metal stirring in the tool running-on and backward slip zones. With an increase in the distance from the welding area in the direction perpendicular to the weld, these temperature changes on the side of the tool backward slip and running-on zones are smoothed.

The values of the maximum temperatures reached during welding at the considered points of installation of thermocouples obtained experimentally and using numerical modelling differ by no more than 5 %. Moreover, the curves describing the nature of temperature changes depending on the time obtained experimentally and theoretically have a similar nature. This indicates the possibility of using computer simulation to estimate the temperature distribution in the welding zone.

The obtained results of the distribution of temperature fields at the periphery of the tool-part contact are in good agreement with the theoretical data existing in the literature, as well as with the data obtained experimentally in this work during butt welding of parts made of the AA5083 aluminum alloy.

Numerical modelling of the distribution of temperature fields during FSW using a thermomechanical model (Abaqus software) taking into account the coupled Euler – Lagrange approach, the Johnson – Cook plasticity model, and the Coulomb friction law was carried out. The results of numerical modelling are proved by the experimental investigation of the distribution of temperature fields when producing a butt welded joint made of the AA5083 aluminum alloy 5 mm thick. The difference between the theoretical and experimental results does not exceed 5 %.

The application of the approach based on the metal mass scaling during numerical modelling of temperature fields by recalculating the metal density and thermal properties allows reducing the time for theoretical calculations by more than one order.

REFERENCES

1. Ishchenko A.Ya., Podelnikov S.V., Poklyatskiy A.G. Friction stir welding of aluminium alloys (Review). *Avtomaticheskaya svarka*, 2007, no. 11, pp. 32–38.
2. Arbegast W.J. Friction stir welding after a decade of development. *Welding Journal*, 2006, vol. 85, no. 3, pp. 28–35.
3. Okamura H., Aota K., Ezumi M. Friction stir welding of aluminum alloy and application to structure. *Journal of Japan Institute of Light Metals*, 2000, vol. 50, no. 4, pp. 166–172. DOI: 10.2464/jilm.50.166.
4. Salloomi K.N., Hussein F.I., Al-Sumaidae S.N.M. Temperature and stress evaluation during three different phases of friction stir welding of AA 7075-T651 alloy. *Modelling and Simulation in Engineering*, 2020, vol. 2020, pp. 1–11. DOI: 10.1155/2020/3197813.
5. Ragab M., Liu H., Yang G.-J., Ahmed M.M.Z. Friction stir welding of 1Cr11Ni2W2MoV martensitic stainless steel: Numerical simulation based on coupled Eulerian Lagrangian approach supported with experimental work. *Applied Science*, 2021, vol. 11, no. 7, pp. 1–6. DOI: 10.3390/app11073049.
6. Chauhan P., Jain R., Pal S.K., Singh S.B. Modeling of defects in friction stir welding using coupled Eulerian and Lagrangian method. *Journal of Manufacturing Processes*, 2018, vol. 34-A, pp. 158–166. DOI: 10.1016/j.jmapro.2018.05.022.
7. Meyghani B., Awang M.B., Emamian S.S., Mohd Nor M.K.B., Pedapati S.R. A Comparison of Different Finite Element Methods in the Thermal Analysis of Friction Stir Welding (FSW). *Metals*, 2017, vol. 7, no. 10, article number 450. DOI: 10.3390/met7100450.
8. Andrade D.G., Leitão C., Dialami N., Chiumenti M., Rodrigues D.M. Modelling torque and temperature in friction stir welding of aluminium alloys. *International Journal of Mechanical Sciences*, 2020, vol. 182, article number 105725. DOI: 10.1016/j.ijmecsci.2020.105725.
9. El-Sayed M.M., Shash A.Y., Mahmou T.S., Rabbou M.A. Effect of friction stir welding parameters on the peak temperature and the mechanical properties of aluminum alloy 5083-O. *Advanced Structured Materials*, 2018, vol. 72, pp. 11–25. DOI: 10.1007/978-3-319-59590-0_2.
10. El-Sayed M.M., Shash A.Y., Abd-Rabou M. Finite element modeling of aluminum alloy AA5083-O friction stir welding process. *Journal of Materials Processing Technology*, 2018, vol. 252, pp. 13–24. DOI: 10.1016/j.jmatprotec.2017.09.008.
11. Patil S., Tay Y.Y., Baratzadeh F., Lankarani H. Modeling of friction-stir butt-welds and its application in automotive bumper impact performance. Part 1. Thermo-mechanical weld process modeling. *Journal of Mechanical Science and Technology*, 2018, vol. 32, no. 6, pp. 2569–2575. DOI: 10.1007/s12206-018-0514-0.
12. Lia K., Jarrara F., Sheikh-Ahmada J., Ozturkb F. Using coupled Eulerian Lagrangian formulation for accurate modeling of the friction stir welding process. *Procedia Engineering*, 2017, vol. 207, pp. 574–579. DOI: 10.1016/j.proeng.2017.10.1023.
13. Mohammad A.A., Avik S., Reza A.B., Hongtao D. An efficient coupled Eulerian-Lagrangian finite element model for friction stir processing. *The International Journal of Advanced Manufacturing Technology*, 2019, vol. 101, pp. 1495–1508. DOI: 10.1007/s00170-018-3000-z.
14. Malik V., Sanjeev N.K., Suresh H.S., Kailas S.V. Investigations on the effect of various tool pin profiles in

friction stir welding using finite element simulations. *Procedia Engineering*, 2014, vol. 97, pp. 1060–1068. DOI: 10.1016/j.proeng.2014.12.384.
15. Ranjole C., Singh V.P., Kuriachen B., Vineesh K.P. Numerical prediction and experimental investigation of temperature, residual stress and mechanical properties of dissimilar friction-stir welded AA5083 and AZ31 alloys. *Arabian Journal for Science and Engineering*, 2022, vol. 47, pp. 16103–16115. DOI: 10.1007/s13369-022-06808-3.
16. Garcia-Castillo F.A., Reyes L.A., Garza C., Lopez-Botello O.E., Hernandez-Munoz G.M., Zambrano-Robledo P. Investigation of microstructure, mechanical properties, and numerical modeling of Ti6Al4V joints produced by friction stir spot welding. *Journal of Materials Engineering and Performance*, 2020, vol. 29, no. 6, pp. 4105–4116. DOI: 10.1007/s11665-020-04900-z.
17. Salloomi K.N. Fully coupled thermomechanical simulation of friction stir welding of aluminum 6061-T6 alloy T-joint. *Journal of Manufacturing Processes*, 2019, vol. 45, pp. 746–754. DOI: 10.1016/j.jmapro.2019.06.030.
18. Kamal M., Shah M., Ahmad N., Wani O.I., Sahari J. Study of crashworthiness behavior of thin-walled tube under axial loading by using computational mechanics. *International Journal of Materials and Metallurgical Engineering*, 2016, vol. 10, no. 8, pp. 1170–1175. DOI: 10.5281/zenodo.1130389.
19. Chao Y.J., Liu S., Chien C.H. Friction stir welding of AL 6061-T6 thick plates: Part II. Numerical modeling of the thermal and heat transfer phenomena. *Journal of the Chinese Institute of Engineers*, 2008, vol. 31, no. 5, pp. 769–779. DOI: 10.1080/02533839.2008.9671431.
20. Wang C., Deng J., Dong C., Zhao Y. Numerical simulation and experimental studies on stationary shoulder friction stir welding of aluminum alloy t-joint. *Frontiers in Materials*, 2022, vol. 9, pp. 1–8. DOI: 10.3389/fmats.2022.898929.

СПИСОК ЛИТЕРАТУРЫ

1. Ищенко А.Я., Подъельников С.В., Покляцкий А.Г. Сварка трением с перемешиванием алюминиевых сплавов (обзор) // Автоматическая сварка. 2007. № 11. С. 32–38.
2. Arbegast W.J. Friction stir welding after a decade of development // Welding Journal. 2006. Vol. 85. № 3. P. 28–35.
3. Okamura H., Aota K., Ezumi M. Friction stir welding of aluminum alloy and application to structure // Journal of Japan Institute of Light Metals. 2000. Vol. 50. № 4. P. 166–172. DOI: 10.2464/jilm.50.166.
4. Salloomi K.N., Hussein F.I., Al-Sumaidae S.N.M. Temperature and stress evaluation during three different phases of friction stir welding of AA 7075-T651 alloy // Modelling and Simulation in Engineering. 2020. Vol. 2020. P. 1–11. DOI: 10.1155/2020/3197813.
5. Ragab M., Liu H., Yang G.-J., Ahmed M.M.Z. Friction stir welding of 1Cr11Ni2W2MoV martensitic stainless steel: Numerical simulation based on coupled Eulerian Lagrangian approach supported with experimental work // Applied Science. 2021. Vol. 11. № 7. P. 1–6. DOI: 10.3390/app11073049.
6. Chauhan P., Jain R., Pal S.K., Singh S.B. Modeling of defects in friction stir welding using coupled Eulerian and Lagrangian method // Journal of Manufacturing Processes. 2018. Vol. 34-A. P. 158–166. DOI: 10.1016/j.jmapro.2018.05.022.
7. Meyghani B., Awang M.B., Emamian S.S., Mohd Nor M.K.B., Pedapati S.R. A Comparison of Different Finite Element Methods in the Thermal Analysis of Friction Stir Welding (FSW) // Metals. 2017. Vol. 7. № 10. Article number 450. DOI: 10.3390/met7100450.
8. Andrade D.G., Leitão C., Dialami N., Chiumenti M., Rodrigues D.M. Modelling torque and temperature in friction stir welding of aluminium alloys // International Journal of Mechanical Sciences. 2020. Vol. 182. Article number 105725. DOI: 10.1016/j.ijmecsci.2020.105725.
9. El-Sayed M.M., Shash A.Y., Mahmou T.S., Rabbou M.A. Effect of friction stir welding parameters on the peak temperature and the mechanical properties of aluminum alloy 5083-O // Advanced Structured Materials. 2018. Vol. 72. P. 11–25. DOI: 10.1007/978-3-319-59590-0_2.
10. El-Sayed M.M., Shash A.Y., Abd-Rabou M. Finite element modeling of aluminum alloy AA5083-O friction stir welding process // Journal of Materials Processing Technology. 2018. Vol. 252. P. 13–24. DOI: 10.1016/j.jmatprotec.2017.09.008.
11. Patil S., Tay Y.Y., Baratzadeh F., Lankarani H. Modeling of friction-stir butt-welds and its application in automotive bumper impact performance. Part 1. Thermo-mechanical weld process modeling // Journal of Mechanical Science and Technology. 2018. Vol. 32. № 6. P. 2569–2575. DOI: 10.1007/s12206-018-0514-0.
12. Lia K., Jarrara F., Sheikh-Ahmada J., Ozturkb F. Using coupled Eulerian Lagrangian formulation for accurate modeling of the friction stir welding process // Procedia Engineering. 2017. Vol. 207. P. 574–579. DOI: 10.1016/j.proeng.2017.10.1023.
13. Mohammad A.A., Avik S., Reza A.B., Hongtao D. An efficient coupled Eulerian-Lagrangian finite element model for friction stir processing // The International Journal of Advanced Manufacturing Technology. 2019. Vol. 101. P. 1495–1508. DOI: 10.1007/s00170-018-3000-z.
14. Malik V., Sanjeev N.K., Suresh H.S., Kailas S.V. Investigations on the effect of various tool pin profiles in friction stir welding using finite element simulations // Procedia Engineering. 2014. Vol. 97. P. 1060–1068. DOI: 10.1016/j.proeng.2014.12.384.
15. Ranjole C., Singh V.P., Kuriachen B., Vineesh K.P. Numerical prediction and experimental investigation of temperature, residual stress and mechanical properties of dissimilar friction-stir welded AA5083 and AZ31 alloys // Arabian Journal for Science and Engineering. 2022. Vol. 47. P. 16103–16115. DOI: 10.1007/s13369-022-06808-3.
16. Garcia-Castillo F.A., Reyes L.A., Garza C., Lopez-Botello O.E., Hernandez-Munoz G.M., Zambrano-Robledo P. Investigation of microstructure, mechanical properties, and numerical modeling of Ti6Al4V joints produced by friction stir spot welding // Journal of Materials Engineering and Performance. 2020. Vol. 29. № 6. P. 4105–4116. DOI: 10.1007/s11665-020-04900-z.
17. Salloomi K.N. Fully coupled thermomechanical simulation of friction stir welding of aluminum 6061-T6 alloy

T-joint // Journal of Manufacturing Processes. 2019. Vol. 45. P. 746–754. DOI: 10.1016/j.jmapro.2019.06.030.
18. Kamal M., Shah M., Ahmad N., Wani O.I., Sahari J. Study of crashworthiness behavior of thin-walled tube under axial loading by using computational mechanics // International Journal of Materials and Metallurgical Engineering. 2016. Vol. 10. № 8. P. 1170–1175. DOI: 10.5281/zenodo.1130389.
19. Chao Y.J., Liu S., Chien C.H. Friction stir welding of AL 6061-T6 thick plates: Part II. Numerical modeling of the thermal and heat transfer phenomena // Journal of the Chinese Institute of Engineers. 2008. Vol. 31. № 5. P. 769–779. DOI: 10.1080/02533839.2008.9671431.
20. Wang C., Deng J., Dong C., Zhao Y. Numerical simulation and experimental studies on stationary shoulder friction stir welding of aluminum alloy t-joint // Frontiers in Materials. 2022. Vol. 9. P. 1–8. DOI: 10.3389/fmats.2022.898929.

Численное моделирование температурных полей при сварке трением с перемешиванием алюминиевого сплава АА5083

Зыбин Игорь Николаевич*[1], кандидат технических наук, доцент,
доцент кафедры «Технологии соединения и обработки материалов»
Антохин Михаил Сергеевич[2], магистрант кафедры «Технологии соединения и обработки материалов»
Калужский филиал Московского государственного технического университета имени Н.Э. Баумана, Калуга (Россия)

***E-mail: igor.zybin@mail.ru**

[1]ORCID: https://orcid.org/0000-0002-5738-4231
[2]ORCID: https://orcid.org/0000-0002-8043-1606

Поступила в редакцию 12.12.2022 *Принята к публикации 30.01.2023*

Аннотация: Одним из важных параметров, обеспечивающих получение сварного соединения при сварке трением с перемешиванием без дефектов сплошности, является обеспечение в зоне соединения металлов требуемой температуры. При экспериментальном определении температуры непосредственно в зоне перемешивания металлов с помощью термопар возникают значительные трудности. В связи с этим актуальным представляется использование численных методов, описывающих распределение температурных полей при сварке трением с перемешиванием. В работе выполнено численное моделирование температурных полей при сварке трением с перемешиванием на основе метода конечных элементов с использованием программного обеспечения Abaqus/Explicit. Моделирование выполнялось на основе связанного подхода Эйлера – Лагранжа, модели пластичности материала Джонсона – Кука и закона трения Кулона. С помощью метода конечных элементов построены модели детали, подложки и инструмента с учетом их теплофизических свойств. Для сокращения времени вычислений использовался подход масштабирования массы путем пересчета плотности материала и его тепловых свойств. Были подобраны коэффициенты масштабирования теплоемкости и массы материала для выбранных параметров режима сварки. Для оценки адекватности результатов численного моделирования температурных полей при сварке трением с перемешиванием были проведены экспериментальные исследования температурных полей с использованием термопар. Показана возможность численного моделирования температурных полей при сварке трением с перемешиванием с помощью связанного подхода Эйлера – Лагранжа и программного обеспечения Abaqus/Explicit. Благодаря применению подхода, связанного с масштабированием массы материала, время вычислений сокращено более чем в 10 раз.

Ключевые слова: сварка трением с перемешиванием; АА5083; связанный подход Эйлера – Лагранжа; численное моделирование температурных полей.

Для цитирования: Зыбин И.Н., Антохин М.С. Численное моделирование температурных полей при сварке трением с перемешиванием алюминиевого сплава АА5083 // Frontier Materials & Technologies. 2023. № 1. С. 23–32. DOI: 10.18323/2782-4039-2023-1-23-32.